Analytical Methods

ROYAL SOCIETY
OF CHEMISTRY

PAPER

Check for updates

Development and validation of a real-time microelectrochemical sensor for clinical monitoring of tissue oxygenation/perfusion†

Gama Theophile Gnahoré,*[a] Jack L. Kelly,[b] Saidhbhe L. O'Riordan,[a] Fiachra B. Bolger,[a] Michelle M. Doran,[a] Michelle Sands[a] and John P. Lowry ⓘD *[a]

Oxygen is of critical importance to tissue viability and there is increasing demand for its reliable real-time clinical monitoring in order to prevent, diagnose, and treat several pathological disorders, including hypoxia, stroke and reperfusion injury. Herein we report the development and characterisation of a prototype clinical O_2 sensor, and its validation *in vivo*, including proof-of-concept monitoring in patients undergoing surgery for carpal tunnel release. An integrated platinum-based microelectrochemical device was custom designed and controlled using a miniaturised telemetry-operated single channel clinical potentiostat. The *in vitro* performance of different sensor configurations is presented, with the best sensor design (S_2) displaying appropriate linearity ($R^2 = 0.994$) and sensitivity (0.569 ± 0.022 nA μM^{-1}). Pre-clinical validation of S_2 was performed in the hind limb muscle of anaesthetised rats; tourniquet application resulted in a significant rapid decrease in signal ($90 \pm 27\%$, [ΔO_2] *ca.* 140 ± 18 μM), with a return to baseline within a period of *ca.* 3 min following tourniquet release. Similar trends were observed in the clinical study; an immediate decrease in signal ($39 \pm 3\%$, [ΔO_2] *ca.* 30 ± 20 μM), with basal levels re-established within 2 min of tourniquet release. These results confirm that continuous real-time monitoring of dynamic changes in tissue O_2 can serve as an indicator of reperfusion status in patients undergoing carpal tunnel surgery, and suggests the potential usefulness of the developed microelectrochemical sensor for other medical conditions where clinical monitoring of O_2 and perfusion is important.

1. Introduction

Oxygen is of critical importance to cell and tissue viability. Consequently, abnormal fluctuations in O_2 levels can lead to a number of ischemic conditions including hypoxia, cardiomyopathy, stroke, reperfusion injury, and oxygen toxicity.[1–4] It is, therefore, important to be able to measure and/or monitor tissue O_2 levels for the prevention, diagnosis, and treatment of these pathological disorders. To date, several methods for the *in vivo* monitoring of O_2 have been reported. These include imaging techniques such as functional magnetic resonance imaging (fMRI), positron emission tomography (PET), near-infrared spectroscopy (NIR), and diffuse reflectance spectroscopy (DRS).[5–10] Although these methods are non-invasive, they

have limitations depending on the technique,[11–13] such as the use of intravenous reporter molecules trapped in the tissue, calibrations limited to hypoxic conditions, and the output of an average or unreliable tissue O_2 value. Another non-invasive method routinely used in clinical monitoring is pulse oximetry.[14,15] To measure O_2 saturation, this technique exploits the difference in light absorption properties between reduced and oxygenated haemoglobins and relies on the patient's normal pulse waveform,[16,17] which is a function of perfusion. Therefore, poor perfusion can result in erratic or absent readings. For example, it has been found that pulse oximetry is unreliable in conditions such as hypotension, hypothermia, cold extremities, cardiopulmonary bypass, low cardiac output or hypovolaemia.[18,19]

Electrochemical sensors have also been successfully used for clinical O_2 measurement. These devices have predominantly been developed based on the principal of the Clark electrode,[20] where O_2 is reduced at a cathodically polarised Pt surface and the resulting faradaic current is taken to be proportional to the concentration of O_2.[21] For example, the Integra Licox® sensor (Integra Life Sciences Corporation, Plainsboro, New Jersey) employs Clark electrode technology to measure continuous tissue O_2 levels in patients with traumatic brain injury (TBI).[22,23]

[a]Maynooth University Department of Chemistry, The Kathleen Lonsdale Institute for Human Health Research, Maynooth, Co. Kildare, Ireland. E-mail: John.Lowry@mu.ie; GamaTheophile.Gnahore@mu.ie

[b]Department of Plastic and Reconstructive Surgery, Galway University Hospitals, Galway, Ireland

† This study is dedicated to the memory of Dr John Scanlan, Director of Commercialisation at Maynooth University, a key supporter of the clinical sensors project who sadly passed away to cancer in 2019.

However, calibration can take up to an hour resulting in delayed output of a signal reflecting local O_2 levels.[24–27] Thus, depending on the clinical application, there is still a recognised unmet need for analytical methodologies capable of measuring tissue oxygenation/perfusion with appropriate sensitivity and temporal resolution in order to assist physicians in diagnostic and treatment decision-making. The information provided by this technology may also have a broader impact by facilitating a better understanding of the physiological role of O_2 and its potential use in medical therapy.[28]

We have previously reported the successful use of implantable microelectrodes developed for real-time monitoring of O_2 levels in cerebral tissue of freely-moving rodents,[29–31] and demonstrated that such measurements are a reliable index of changes in blood flow.[29,32] In this study, we used our experience of developing real-time neurochemical sensors to design and validate a new integrated microelectrochemical sensor device for *in situ* clinical monitoring of peripheral tissue O_2 and perfusion. The technology was characterised both *in vitro* and *in vivo* before performing a proof-of-concept clinical study to monitor rapid continuous dynamic changes in oxygenation in patients undergoing surgery for carpal tunnel release.

2. Experimental

2.1 Chemicals

Sodium chloride (NaCl), sodium hydroxide (NaOH) and sodium hydrogen phosphate (Na_2HPO_4), used to make the phosphate buffered saline (PBS), were of analytical grade and purchased from Sigma-Aldrich Ireland (Dublin). All solutions were prepared using Milli-Q® water (Milli-Q® Direct Water Purification System, Merck).

2.2 Sensor fabrication

Two geometries of Pt electrodes (*Pt-disk* and *Pt-cylinder*) were constructed using *ca.* 5 cm lengths of Teflon®-insulated Pt/Ir (90%/10%) wire (125 μm bare diameter, 175 μm coated diameter (5T); Advent Research Materials, Suffolk, UK). 2 cm of Teflon® was removed from one end of the wire and soldered into a gold clip for electrical conductivity and rigidity. The opposite end of the wire was cut with a sharp scalpel blade to create a disk surface (*Pt-disk*). The *Pt-cylinder* was constructed in a similar manner, except that after the soldering process 1 mm of Teflon® was removed from the opposite end of the wire, which served as the active surface. Two of these electrodes were then combined with the *Pt-disk* electrode and encased in heat shrink tubing parallel to each other. The *Pt-cylinder* electrodes were used as pseudo-reference and auxiliary electrodes (RE, AE), with the *Pt-disk* electrode employed as the working electrode (WE).

Two different sensor configurations (S_1 and S_2) were prepared. As the active surface of the AE and RE is cylindrical, there is a risk of short-circuit if these electrodes are aligned side-by-side, particularly following *in vivo* implantation. Therefore, S_1 was designed by incorporating an electrode spacer in the construction of the device to avoid touching of the exposed electrode surfaces. The spacer was made of plastic using an injection molding (Irish Micro Mouldings Ltd, Galway, Ireland). It incorporated two grooves for AE and RE positioning, with the WE fed through a central cavity such that it protruded *ca.* 0.5 cm. UV adhesive was applied to each end of the spacer to secure the electrodes and to facilitate waterproofing of the device (Fig. 1A). S_2 was constructed without the use of the electrode spacer (Fig. 1B); RE was placed 1.5 mm above the working and auxiliary electrodes, which were positioned beside each other. The ClinOX O_2 sensor was manufactured by Nordson Medical (Clada Medical Devices, Galway, Ireland) following a previously described procedure.[33]

2.3 Instrumentation and software

All *in vitro*, *in vivo* and clinical O_2 measurements were performed using constant potential amperometry (CPA) on a portable telemetry-based battery-operated potentiostat (ISO 13485 compliant) with an in-built A/D converter (Bluebridge Technologies, Dublin, Ireland). Data collection (Microsoft Excel) was performed with a custom designed IEC 62304 compliant IOS App (Bluebridge Technologies) running on an Apple iPad (Bluebridge Technologies). As the amperometric O_2 reduction reaction (−650 mV *vs.* SCE) produces increasing negative cathodic currents with increasing concentration (Fig. 2), data are presented as absolute values (unless otherwise stated) in order to avoid visual confusion with respect to changes (increases/decreases) in O_2 levels. The significance of differences observed was estimated in GraphPad Prism 5 (GraphPad Software Inc., CA, USA) using Student's *t*-tests (two-tailed paired or unpaired where appropriate). All data are expressed as the mean ± standard error (SEM).

2.4 *In vitro* experiments

All amperometric O_2 calibrations (pre- and post-implantation) were carried out in a standard three-electrode glass electrochemical cell containing PBS (20 mL, pH 7.4) as the supporting electrolyte and using the manufactured sensors S_1 and S_2, described in Section 2.2. PBS saturated with N_2 or O_2 was obtained by purging with the respective gas for approximately 1 hour. Calibrations were performed over the O_2 concentration range of 0–125 μM by adding standard aliquots (25 μM) of the O_2-saturated PBS to the cell containing PBS (N_2-saturated). The cell solution was mixed following each aliquot injection using a magnetic stirrer (IKA MST Mini Magnetic stirrer, Lennox Laboratory Supplies Ltd., Dublin, Ireland) and a stirrer bar (5 mm diameter × 10 mm length) for *ca.* 3 s. A N_2 cloud was maintained just above the surface of the solution to avoid a backflow of ambient air into the cell. All *in vitro* experiments were performed at room temperature (23 ± 2 °C) using *Pt-cylinders* as pseudo-reference and auxiliary electrodes, unless otherwise stated. Concentrations were determined from pre-implantation calibration obtained using CPA at −650 mV as this potential has previously been reported to be optimum for the electrochemical reduction of O_2 at Pt-based microelectrodes.[34]
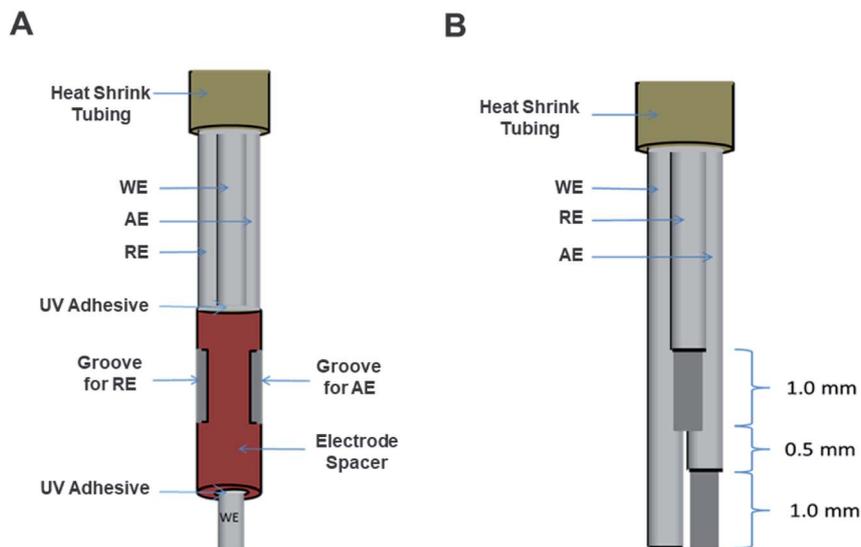
Fig. 1 Schematic representation of the tips of sensors S_1 and S_2 showing the configuration of the Teflon®-insulated Pt/Ir wires used to construct the sensors. In both designs the working electrode (WE) has a disk geometry. (A) S_1 configuration showing the exposed cylindrical surfaces of the reference (RE) and auxiliary electrodes (AE), inserted into opposite grooves of the spacer, with the WE fed through the central cavity. (B) S_2 configuration showing the spatial configuration of the cylindrical surfaces of RE and AE separated by *ca.* 0.5 mm to avoid electrode touching. For construction details see Section 2.2.
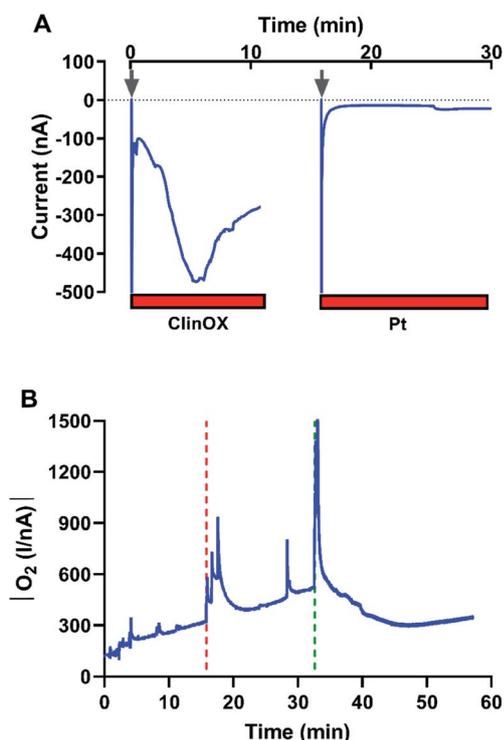
Fig. 2 (A) Current–time profiles for ClinOX and bare Pt microelectrode O_2 sensors in N_2-saturated PBS, pH 7.4. Arrows indicate application of −650 mV (*vs.* Pt RE, Pt AE) O_2 reduction potential. (B) Example of a raw data trace recorded using a ClinOX sensor implanted in the hind limb of an anaesthetised rat (CPA, −650 mV *vs.* Pt RE). Hashed lines represent application (red) and removal (green) of tourniquet. Data presented as absolute values.

2.5 *In vivo* experiments

Male Wistar rats (300–600 g; Charles River Laboratories International, Inc., U.K.) were housed in a temperature and humidity controlled facility with a 12 h light/dark cycle with access *ad libitum* to food and water. The rats were allowed to acclimatise to their new environment for a period of one week prior to sensor implantation. All animal work was carried out with approval from the Maynooth University Research Ethics Committee, and under license in accordance with the European Communities Regulations 2002 (Irish Statutory Instrument 566/2002 – Amendment of Cruelty to Animals Act 1876).

The animals were initially anaesthetised in an induction chamber with the volatile anaesthetic isoflurane (4% in air; Isofluorin® 1000 mg g^{-1}, Vetpharma Animal Health, S.L., Spain) using a Univentor 400 Anaesthesia Unit and Scavenger (AgnTho's AB, Sweden). They were then placed in the supine position on a temperature-controlled heating pad and body temperature maintained at 37 ± 0.5 °C using a rectal probe (Harvard Apparatus; PanLab, Barcelona, Spain). The level of anaesthesia was reduced to 2% and rerouted using a gas routing switch to an anaesthesia mask (AgnTho's AB) which was placed over the nose. After *ca.* 5 min the level of anaesthesia was reduced to a maintenance level of *ca.* 1.5% and checked regularly (pedal withdrawal reflex and tail pinch).

A tourniquet (tie wrap) was then positioned loosely around the base of the hind limb. The sensor was inserted into the muscle *via* a sterile siliconised stainless-steel needle with double wings (16 G × 30 mm, Vygon UK Ltd., MedGuard, Ireland), and once fully implanted the needle was carefully retracted and split in half while maintaining the position of the sensor within the muscle. After application of the applied potential, each animal was given a further 5 min before

Analytical Methods

Paper

experiments were begun in order to ensure that the background current for the sensor was stabilised. Ischemia was then induced by tightening the tourniquet to reduce blood flow which was checked visually by the pallor of the foot. The tourniquet was applied for a maximum period of 10 min. Pre- and post-tourniquet recordings (baselines) were obtained for a similar period of *ca.* 10 min. At the end of this process, the tourniquet was removed and the animal was euthanised by intraperitoneal administration of sodium pentobarbital (Euthanimal – 200 mg mL^{-1}; Bioresource Unit, Maynooth University).

2.6 Sensor sterilisation

The prototype sensors prepared for clinical use were carefully packaged in sealable Tyvek bags (Bemis Healthcare Packaging, Co Offaly, Ireland) following construction and calibration. The bagged sensors were then subjected to gamma irradiation (25 kGy min^{-1}, Synergy Health, Co Mayo, Ireland) in preparation for use in a clinical setting.

2.7 Clinical proof-of-concept study

The prototype clinical sensor S_2 was implanted in patients undergoing surgery for carpal tunnel release. This procedure involves severing the tranverse carpal ligament in the wrist to reduce pressure on the median nerve. Briefly, local anaesthetic (2% lidocaine with 1 : 200 000 adrenaline) was administered along the incision line at the wrist prior to surgery. A small amount of local anaesthetic was used to anaesthetise a small area of the forearm prior to sensor insertion through the skin. An un-inflated tourniquet was applied to the proximal arm above the site of sensor insertion and above the incision site. The sensor was implanted into the extensor muscles of the forearm through the previously anaesthetised skin using a 23 G introductory needle (Vygon UK Ltd., MedGuard, Ireland) that was retracted leaving the device at the recording site. The instrumentation was started and a 5 min baseline period was recorded before tourniquet application (above the site of sensor implantation) and before the commencement of surgery. A further 5 min baseline period was recorded after surgery and tourniquet release. The sensor was then carefully removed from the muscle, and kept for recalibration before disposal. Six patients agreed to participate in this clinical research study, which was carried out with approval from the Maynooth University Research Ethics Committee (BSRESC-2016-001), and the Clinical Research Ethics Committee of Galway University Hospital (C.A.1389). Insurance was provided by Willis Towers Watson (Ireland) Ltd.

3. Results and discussion

3.1 *In vitro* and *in vivo* O_2 measurements

Our initial plan was to perform the clinical study using a previously reported Pt–Pt ClinOX sensor that had been specifically designed and commercially manufactured for clinical application.[33] However, despite *in vitro* and *in vivo* (rodents and pigs) data suggesting potential suitability for clinical application, we

found that the device had a tendency to be unreliable, and hence unsuitable in its current format for clinical use. Fig. 2A shows typical capacitance current data for both the ClinOX sensor and a standard Pt O_2 electrode[34] following application of the O_2 reduction potential. The latter reached a stable baseline current within a couple of minutes, as expected, while the former failed to settle producing a large wandering signal over a similar recording period. Fig. 2B shows *in vivo* data from a ClinOX sensor implanted in the hind limb of an anaesthetised rat (see Section 2.5 for experimental protocol) where the baseline failed to settle, and tourniquet application and removal (hashed lines) resulted in a variable increase in the O_2 signal, despite the decrease in tissue O_2 associated with reduced blood flow (*e.g.* see Fig. 3B). A detailed investigation revealed this to be the result of a combination of poor seals and electrical shorting between electrodes. As such, a new sensor design, S_1 (see Fig. 1A), was configured which incorporated insulated wires and an electrode spacer to avoid shorting.

The electrochemical behavior of S_1 was investigated by performing O_2 calibrations in N_2-saturated PBS (pH 7.4) over the physiologically relevant concentration range 0–125 μM. Both capacitance and faradaic signals were normal with S_1 displaying both good linearity ($R^2 = 0.989$) and sensitivity of 0.38 ± 0.02 nA μM^{-1} ($n = 3$, Fig. 3A). The sensor's performance was then
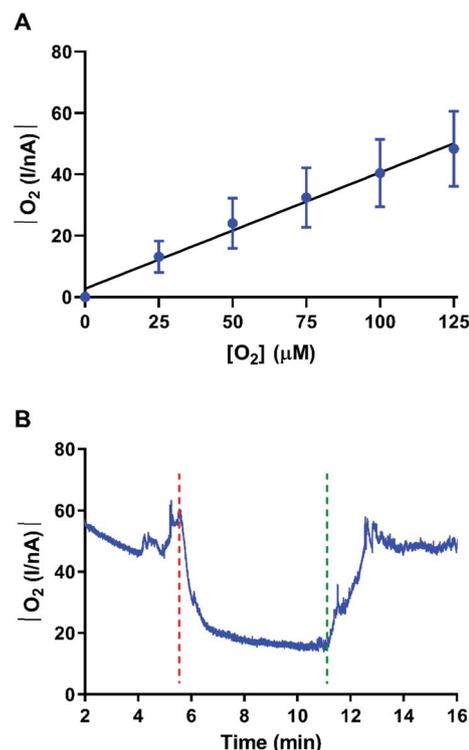
Fig. 3 (A) *In vitro* O_2 calibration plot (0–125 μM, N_2-saturated PBS, pH 7.4) for sensor configuration S_1 ($n = 3$) carried out using constant potential amperometry (CPA) at −650 mV *vs.* Pt RE. Mean background currents subtracted. (B) Raw data trace recorded at sensor S_1 *in vivo* (hind limb of anaesthetised rat). Hashed lines represent application (red) and removal (green) of tourniquet. CPA carried out at −650 mV *vs.* Pt RE.

assessed *in vivo* (rodent hind limb) using the same mild ischemic insult (tourniquet) previously applied to the ClinOX device. In this case, the sensor displayed typical O_2 signal changes associated with ischemia and reperfusion (see Fig. 3B); the current decreased from a baseline of 48.7 nA to a minimum value of 15.8 nA (ΔO_2 *ca.* 80 μM), and then subsequently returned to initial levels (48.4 nA) following tourniquet release. However, on occasion, it was observed that removal of the sensor from the tissue resulted in movement/displacement of the electrode spacer. As this would represent a potential risk with respect to dislodgment in a patient it was decided to further modify the design. Staggering the electrodes resulted in a reproducible design (S_2, see Fig. 1B) where no spacer was required. Injection of each calibration (O_2-saturated PBS) aliquot to the cell resulted in an immediate increase in current, followed by a steady-state plateau (inset, Fig. 4), and yielded similar sensitivity (0.57 ± 0.02 nA μM^{-1}, $n = 14$), and linearity ($R^2 = 0.994$) to that observed with S_1 (see Fig. 4A).

As with S_1, *in vivo* validation using tourniquet application/removal resulted in a rapid decrease in tissue O_2 levels to 9.15

$\pm$ 3.69 nA ($89.8 \pm 27.0\%$, $P = 0.0297$, $n = 3$, 2 animals) from a baseline value of 90.02 ± 17.87 nA, corresponding to an O_2 concentration change of *ca.* 140 ± 18 μM. Tourniquet release resulted in a return to baseline values (98.74 ± 38.15 nA) within a period of *ca.* 4 min, followed by a slight overshoot, most likely due to post-ischemic hyper-perfusion[35–38] (see Fig. 4B). There are two possible explanations for the high baseline SEMs observed. Firstly, one would expect some inter-electrode variability in terms of sensitivity. Secondly, tissue O_2 levels measured can vary depending on implantation parameters such as depth,[39] tissue heterogeneity,[40] and the relative proximity to the local vasculature.[41] These are most likely to be the main contributors, particularly given the *in vitro* reproducibility shown in Fig. 4A. The larger SEM observed for reperfusion may be ascribed to differences in post-ischemic hyper-perfusion. These results clearly demonstrate that S_2 is appropriately sensitive to monitor *in situ* changes in tissue O_2 and suitable for clinical use. A proof-of-concept clinical study was thus designed to test this conclusion.

3.2 Clinical testing

S_2 was implanted in patients undergoing surgery for carpal tunnel release. This procedure was chosen as it requires alterations in perfusion (ischemia/reperfusion) to facilitate severing of the transverse carpal ligament. These alterations are achieved through the application/release of a tourniquet positioned on the upper arm (see Fig. 5 and Section 2.7 – Clinical proof-of-concept study). Typical results from two patients are shown in Fig. 6. Tourniquet application resulted in an immediate decrease in signal from baseline (31.77 ± 8.01 nA, $n = 5$), reaching a minimum of 18.64 ± 3.94 nA ($39.2 \pm 3.3\%$, $P < 0.05$) after 2.38 ± 0.52 min. Return to baseline (34.51 ± 10.28 nA, $P > 0.63$) was typically achieved within 2 min of tourniquet release; the average duration of the procedure, as defined by tourniquet application/release, was 5.56 ± 0.81 min. This data highlights
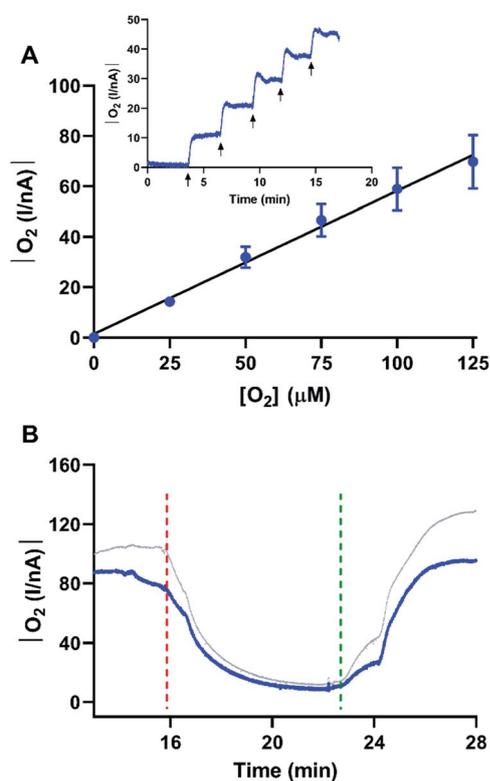
Fig. 4 (A) *In vitro* O_2 calibration plot (0–125 μM) for sensor configuration S_2 ($n = 14$). CPA was carried out at −650 mV *vs.* Pt RE in N_2-saturated PBS (pH 7.4). Mean background currents subtracted. (Inset) Typical raw data trace (current–time) showing sequential step increases in signal for injection of each O_2 concentration (25 μM). Arrows represent point of addition for each aliquot. (B) Average (±SEM, gray) O_2 current response recorded from sensor S_2 implanted in the hind limb of anaesthetised rats ($n = 3$, 2 animals). Hashed lines represent application (red) and removal (green) of tourniquet. Blue and gray traces represent the mean O_2 response and SEM, respectively. CPA carried out at −650 mV *vs.* Pt RE.
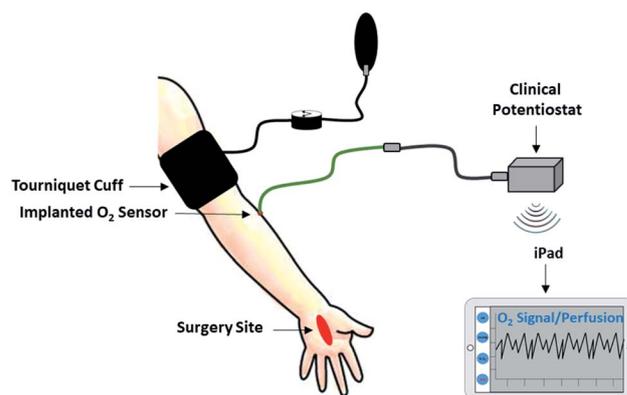
Fig. 5 Schematic diagram illustrating the setup used for the real-time monitoring of tissue O_2/perfusion during carpal tunnel release surgery. The microelectrochemical sensor (S_2) implanted into the forearm is connected to a miniaturised battery-operated single channel potentiostat. Circulation was stopped (and restored) prior to (and after) surgery by using a tourniquet cuff. The O_2 signals were wirelessly transmitted to an Apple iPad for visualisation.
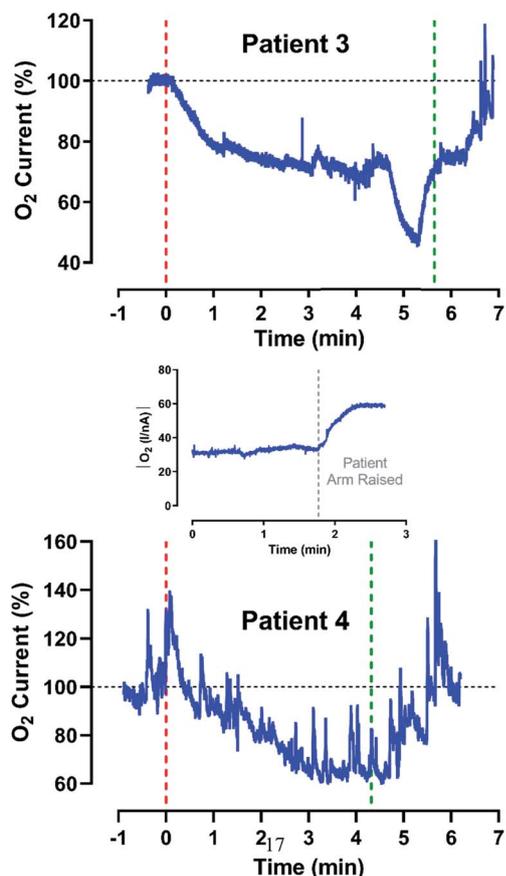
Fig. 6 Examples of raw data traces from S_2 sensors (CPA, -650 mV *vs.* Pt RE) implanted in patients undergoing surgery for carpal tunnel release. Hashed lines represent application (red) and removal (green) of tourniquet. Data normalised to pre-tourniquet baseline current. (Inset) Typical example of a rapid change in absolute O_2 signal associated with repositioning of a patient's arm (hashed grey line) prior to commencement of the surgical procedure.

the ability of the prototype sensor to monitor physiologically relevant rapid changes in perfusion over the course of a short clinical procedure. It is also noteworthy that, on occasion, adjustment of the position of the patient's arm was required prior to tourniquet application, and this also produced fast changes in perfusion that were detected by the sensor (see Fig. 6 inset). The estimated change in O_2 concentration, based on *in vitro* pre-calibration curves, was found to be *ca.* 30 ± 21 μM. In units of pressure (mmHg), commonly used to represent clinical O_2 levels,[34,42–44] this corresponds to 23 ± 16 mmHg. Several of the S_2 sensors were re-calibrated 18 days after the clinical procedure. The sensitivity was found to have decreased from 0.44 ± 0.03 nA μM^{-1} to 0.28 ± 0.02 nA μM^{-1} ($n = 4$, $R^2 = 0.98$, $P = 0.0136$). Given that previous *in vitro* biocompatibility experiments performed in protein, lipid and brain tissue preparations,[34] and *in vivo* characterisation in rodents,[33,45,46] suggest small non-significant changes in O_2 sensitivity at Pt electrodes, it is possible that this may have resulted from the mechanical manipulation associated with removal from the patient. Indeed, longitudinal studies[34] suggest that this type of sensor should be

viable for at least several days following implantation, and possibly longer, and opens the potential for use in longer surgical procedures, and subsequent recovery.

4.   Conclusions

The aim of the present study was to design and validate an integrated microelectrochemical sensor device suitable for real-time monitoring of peripheral tissue O_2 in patients undergoing carpal release surgery. To accomplish this goal, different Clark-type O_2 sensors were procured (ClinOX) and manufactured in-house (sensors S_1 and S_2). The *in vivo* characterisation of ClinOX and S_1 using a mild ischemic insult (tourniquet) highlighted that these sensors were not reliable for clinical use. Whilst the former produced high capacitive currents that failed to settle, the latter showed movement/displacement of the electrode spacer following removal from rodent hind limb. S_2, which involved a staggered electrode configuration, was constructed to address these issues and thus enable tissue O_2 monitoring in humans. *In vitro* calibration data confirmed appropriate sensitivity and rapid response characteristics, which were subsequently supported by *in vivo* experiments performed in the hind limb of anaesthetised rats using tourniquet application and removal. These results paved the way for application of the prototype sensor in a clinical research study involving patients undergoing carpal tunnel surgery, where similar real-time dynamic changes in tissue O_2 were observed. Success in these proof-of-concept studies suggests that the developed device could potentially find application in other medical conditions (*e.g.* free flap surgery) where monitoring of peripheral tissue oxygenation/perfusion could improve the procedure and patient outcome.

Conflicts of interest

There are no conflicts to declare.

Acknowledgements

References

1 A. C. Kulkarni, P. Kuppusamy and N. Parinandi, *Antioxid. Redox Signaling*, 2007, **9**, 1717–1730.
2 V. K. Kutala, M. Khan, M. G. Angelos and P. Kuppusamy, *Antioxid. Redox Signaling*, 2007, **9**, 1193–1206.
3 J. Nortje and A. K. Gupta, *Br. J. Anaesth.*, 2006, **97**, 95–106.
4 U. K. Rohlwink and A. A. Figaji, *Child's Nerv. Syst.*, 2010, **26**, 453–464.
5 M. E. Raichle, *Proc. Natl. Acad. Sci. U. S. A.*, 1998, **95**, 765–772.
6 Y. Hoshi, *Int. Rev. Neurobiol.*, 2005, **66**, 237–266.

7 L. M. Foley, P. Picot, R. T. Thompson, M. J. Yau and M. Brauer, *Magn. Reson. Med.*, 2003, **50**, 976–983.

8 A. A. Stratonnikov and V. B. Loschenov, *J. Biomed. Opt.*, 2001, **6**, 457–467.

9 E. E. Verwer, R. Boellaard and A. A. van der Veldt, *World J. Clin. Oncol.*, 2014, **5**, 824–844.

10 S. S. Taylor DE, *New Horiz.*, 1996, **4**, 420–425.

11 J. D. Chapman, R. F. Schneider, J. L. Urbain and G. E. Hanks, *Semin. Radiat. Oncol.*, 2001, **11**, 47–57.

12 C. Baudelet and B. Gallez, *Magn. Reson. Med.*, 2002, **48**, 980–986.

13 D. Zhao, L. Jiang, E. W. Hahn and R. P. Mason, *Magn. Reson. Med.*, 2009, **62**, 357–364.

14 G. Tusman, S. H. Bohm and F. Suarez-Sipmann, *Anesth. Analg.*, 2017, **124**, 62–71.

15 M. W. Wukitsch, M. T. Petterson, D. R. Tobler and J. A. Pologe, *J. Clin. Monit.*, 1988, **4**, 290–301.

16 A. Jubran and M. J. Tobin, *Chest*, 1990, **97**, 1420–1425.

17 J. T. Comber and B. L. Lopez, *Am. J. Emerg. Med.*, 1996, **14**, 16–18.

18 J. W. Severinghaus and M. J. Spellman Jr, *Anesthesiology*, 1990, **73**, 532–537.

19 J. Ibanez, J. Velasco and J. M. Raurich, *Intensive Care Med.*, 1991, **17**, 484–486.

20 L. C. Clark Jr and C. Lyons, *Ann. N. Y. Acad. Sci.*, 1962, **102**, 29–45.

21 I. M. Kolthoff and H. A. Laitinen, *Science*, 1940, **92**, 152–154.

22 C. Stewart, I. Haitsma, Z. Zador, J. C. Hemphill 3rd, D. Morabito, G. Manley 3rd and G. Rosenthal, *Neurosurgery*, 2008, **63**, 1159–1164.

23 R. P. Martini, S. Deem and M. M. Treggiari, *Respir. Care*, 2013, **58**, 162–172.

24 L. B. Ngwenya, J. F. Burke and G. T. Manley, *Respir. Care*, 2016, **61**, 1232–1244.

25 K. Purins, P. Enblad, B. Sandhagen and A. Lewen, *Acta Neurochir.*, 2010, **152**, 681–688.

26 J. Dengler, C. Frenzel, P. Vajkoczy, S. Wolf and P. Horn, *Intensive Care Med.*, 2011, **37**, 1809–1815.

27 J. A. Green, D. C. Pellegrini, W. E. Vanderkolk, B. E. Figueroa and E. A. Eriksson, *Neurocrit. Care*, 2013, **18**, 20–25.

28 H. B. Stone, J. M. Brown, T. L. Phillips and R. M. Sutherland, *Radiat. Res.*, 1993, **136**, 422–434.

29 F. B. Bolger and J. P. Lowry, *Sensors*, 2005, **5**, 473–487.

30 J. P. Lowry, K. Griffin, S. B. McHugh, A. S. Lowe, M. Tricklebank and N. R. Sibson, *NeuroImage*, 2010, **52**, 549–555.

31 J. Kealy, R. Bennett and J. P. Lowry, *J. Neurosci. Methods*, 2013, **215**, 110–120.

32 J. P. Lowry, M. G. Boutelle and M. Fillenz, *J. Neurosci. Methods*, 1997, **71**, 177–182.

33 N. J. Finnerty and F. B. Bolger, *Bioelectrochemistry*, 2018, **119**, 124–135.

34 F. B. Bolger, R. Bennett and J. P. Lowry, *Analyst*, 2011, **136**, 4028–4035.

35 L. Xiang, P. Yu, M. Zhang, J. Hao, Y. Wang, L. Zhu, L. Dai and L. Mao, *Anal. Chem.*, 2014, **86**, 5017–5023.

36 S. Kimura, K. Matsumoto, K. Mineura and T. Itoh, *J. Neurol. Sci.*, 2007, **258**, 60–68.

37 T. M. Sundt and A. G. Waltz, *Circ. Res.*, 1971, **28**, 426–433.

38 L. Symon, J. C. Ganz and N. W. Dorsch, *Brain*, 1972, **95**, 265–278.

39 H. Baumgärtl, U. Heinrich and D. W. Lübbers, *Pflügers Archiv*, 1989, **414**, 228–234.

40 D. W. Lübbers and H. Baumgärtl, *Kidney Int.*, 1997, **51**, 372–380.

41 J. B. Zimmerman, R. T. Kennedy and R. M. Wightman, *J. Cereb. Blood Flow Metab.*, 1992, **12**, 629–637.

42 N. Offenhauser, K. Thomsen, K. Caesar and M. Lauritzen, *J. Physiol.*, 2005, **565**, 279–294.

43 J. Lecoq, P. Tiret, M. Najac, G. M. Shepherd, C. A. Greer and S. Charpak, *J. Neurosci.*, 2009, **29**, 1424–1433.

44 H. Piilgaard and M. Lauritzen, *J. Cereb. Blood Flow Metab.*, 2009, **29**, 1517–1527.

45 J. P. Lowry, M. G. Boutelle, R. D. O'Neill and M. Fillenz, *Analyst*, 1996, **121**, 761–766.

46 M. E. Gray, J. R. K. Marland, C. Dunare, E. O. Blair, J. Meehan, A. Tsiamis, I. H. Kunkler, A. F. Murray, D. Argyle, A. Dyson, M. Singer and M. A. Potter, *Am. J. Physiol.: Gastrointest. Liver Physiol.*, 2019, **317**, G242–G252.